Pergamon

Bioorganic & Medicinal Chemistry 7 (1999) 517–527

BIOORGANIC & MEDICINAL CHEMISTRY

# *N*-2-(Azol-1(2)-yl)ethyliminodiacetic Acids: A Novel Series of Gd(III) Chelators as $T_2$ Relaxation Agents for Magnetic Resonance Imaging

Pilar López,[a] Christa G. Seipelt,[a] Patrick Merkling,[b] Laszlo Sturz,[b] José Álvarez,[c] Andreas Dölle,[b] Manfred D. Zeidler,[b] Sebastián Cerdán[c] and Paloma Ballesteros[a,*]

[a]*Dpto. Química Orgánica y Biología, Facultad de Ciencias, UNED, Senda del Rey s/n, 28040, Madrid, Spain*
[b]*Institut für Physikalische Chemie, Rheinisch-Westfälische Technische Hochschule, D-52056 Aachen, Germany*
[c]*Instituto de Investigaciones Biomédicas CSIC, c/ Arturo Duperier 4, 28029 Madrid, Spain*

Received 7 August 1998; accepted 6 November 1998

**Abstract**—The synthesis, physicochemical properties, and toxicological implications of a novel series of *N*-2-(azol-1(2)-yl)ethyliminodiacetic acids, useful as contrast agents for magnetic resonance imaging are reported. Compounds were prepared by alkylation of methyl iminodiacetate with *N*-2-bromoethylazoles and subsequent hydrolysis. Stability constants of the corresponding Gd(III) complexes and $T_1$ and $T_2$ relaxivities were determined and interpreted in terms of optimized geometries obtained by semiempirical PM3 calculations. Compounds show increased $T_2$ relaxivity and decreased toxicity in vitro as compared to EDTA-Gd(III) complexes.


## Introduction

Magnetic resonance imaging (MRI) as routinely employed in clinical settings often requires the use of paramagnetic ion chelates as contrast agents.[1–3] Gd(III) remains as the optimal paramagnetic ion for this purpose because of its high electronic spin ($S = 7/2$), relatively slow electronic relaxation rate and exchange labile hydration sphere. However, free Gd(III) is toxic in vitro and in vivo, a circumstance which has prompted research for chelating agents able to minimize its toxicity and optimize its relaxivity properties. Chelating agents developed previously for this purpose included a series of poliaminopolicarboxylic acid derivatives and a family of macrocyclic ligands.[2,4] Four of these compounds have already been approved for clinical use; Gd-diethylenetriaminepentaacetic acid (Gd-DTPA$^{2-}$), Gd-1,4,7,10-tetra-azacyclododecane-1,4,7,10-tetraacetic acid (Gd-DOTA$^{2-}$), Gd-10-(2-hydroxy-propyl)-1,4,7,10-tetraazacyclododecane-1,4,7-triacetic acid (Gd-HPDO3A), and Gd-diethyelenetriamine-*N*,*N*′,*N*″-triacetic acid-*N*,*N*″bis(methylamide) (Gd-H3DTPA-BMA). However, the design of new chelate molecules to improve relaxivity, decrease toxicity, achieve higher organ selectivity or optimize image quality in specific applications constitutes an active area of research.[5–7] This study reports the syntheses, physicochemical characterization, and toxicological properties of a novel series of chelating agents containing heterocyclic rings.

Chelating properties of complexones are well documented.[8] The presence of one or several moieties of iminodiacetic acid (IDA) allow these compounds to form tridentate or higher order coordination complexes with almost all cations, giving chelate rings. Complexones have been used in the quantitative analyses of metal ions, the complexation of heavy metals in nuclear medicine[9] and more recently as contrast agents in magnetic resonance imaging.[10,11] In general, chemical structure of the known complexones includes carboxy, hydroxy or amino groups in addition to one or more iminodiacetic moieties. However, in spite of the high capability of heterocyclic rings as nitrogen-donor ligands,[12–14] few complexones have incorporated yet such rings in their structure. Some 2,2′-bipyridine tetraacetic acid derivatives were proposed as luminescent makers for bioaffinity assays or more recently, even as contrast agents for MRI.[15–18] Our previous experience on azole-containing ligands[19–21] prompted us to further explore the role of nitrogen based heterocycles as additional ligands in complexone structures.

We synthesized complexones **1–4** and evaluated their physicochemical and toxicological properties using IDA or ethylenediamine-*N*,*N*,*N*′,*N*′-tetraacetic acid (EDTA)

*Corresponding author. Fax: +34-1-398-6697.

0968-0896/99/$ - see front matter 
*PII:* S0968-0896(98)00273-9

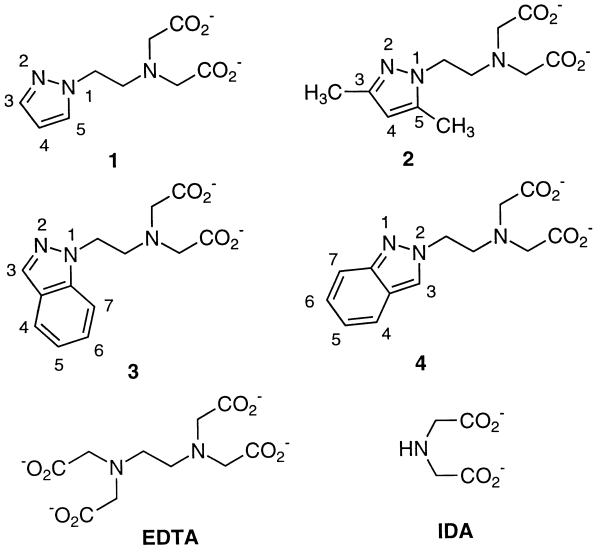


**Chart 1.**

as well characterized reference compounds. The Gd(III) complexes of **3** and **4** display improved $T_2$ relaxivity and lower toxicity in vitro than EDTA-Gd(III). These circumstances make them potentially useful in MRI applications requiring $T_2$ enhancement as the imaging of flow and perfusion.[22]

## Results

### Syntheses of heterocyclic complexones

*N*-2-Bromoethylazoles **8–11** (Scheme 1) were prepared by reaction of the corresponding azoles **5–7** with an excess of 1,2-dibromoethane using liquid–liquid phase transfer catalysis. Although compounds **8** and **9** have been described previously[23,24] we studied in more detail this reaction to optimize conditions preventing the formation of undesirable side vinyl- and bis-derivatives (Table 1).

Bis-azolylethanes were identified in the $^1$H NMR spectra of the reaction crudes by comparison with the previously reported resonances.[25] In the case of indazole **7**, only the 2-substituted isomer of the vinyl derivative was formed in this reaction. Subsequent alkylation with *N*-2-bromoethylazoles to obtain the corresponding methyl *N*-2-(azol-1(2)yl) ethyliminodiacetates **12–15**, was performed using two moles of methyl iminodiacetate[26] to trap the HBr formed in the alkylation process.[27] The methyl *N*-2-(azol-1(2)yl) ethyliminodiacetate hydrobromide was recycled by prior basification with $Na_2CO_3$. The free complexones **1–4** and **16** were obtained by basic or acid hydrolysis. Structures of the diesters and the diacid salts were established by elemental analyses and spectroscopic methods. $^1$H and $^{13}$C NMR spectra were assigned on the basis of previous data.[19–21]

### Heterocyclic complexones as magnetic resonance relaxation agents

Figure 1 shows the effects of increasing Gd(III) concentrations on the linewidth and chemical shift of the water signal in the absence and presence of compounds **1–4** or EDTA. Increasing concentrations of Gd(III) caused increased line broadening and downfield shifts of the water signal. For the same concentration of complexones and Gd(III), the water linewidth was broader with complexones **1–4** than in EDTA. These results suggested that the Gd(III) complexes of compounds **1–4**

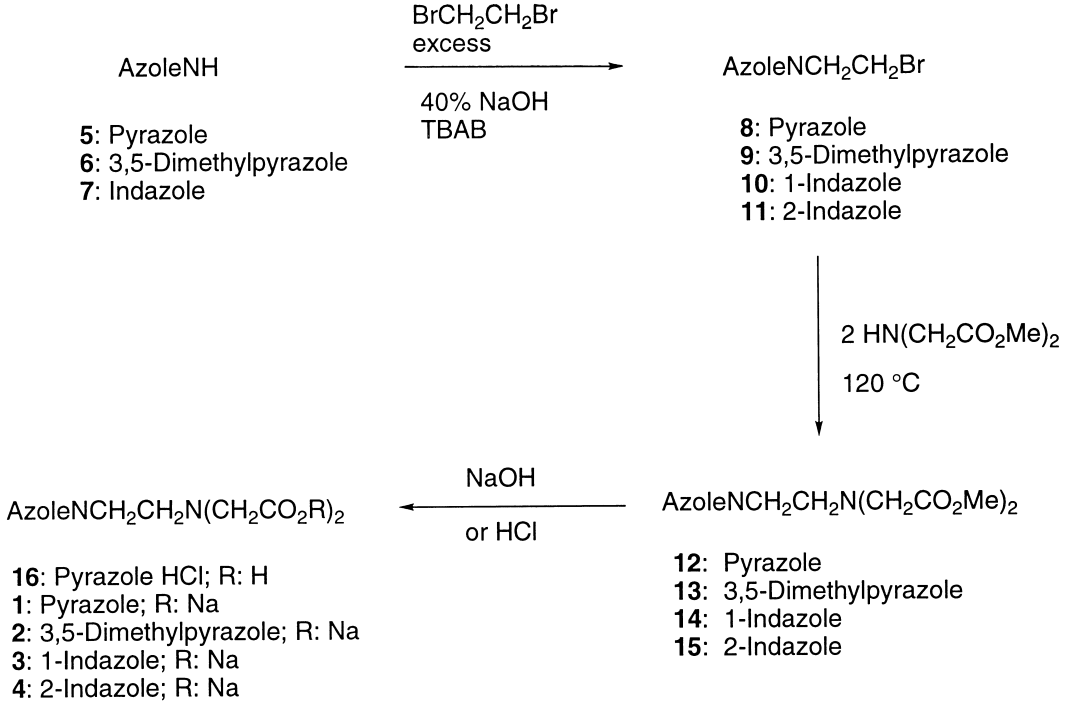


**Scheme 1.**

**Table 1.** Results obtained in the reaction of azoles **5–7** with 1,2-dibromoethane

| Azole | Reaction conditions | Bromoethylazole (%) | Vinylazole (%) | Bis-azolylethane (%) |
|---|---|---|---|---|
| **5** | 24 h/rt | **8**: 90[a]; 72[b] | Traces[a] | Traces[a] |
| **6** | 1 h/reflux | **9**: 60[a]; 42[b] | 10[a] | 30[a] |
| **7** | 24 h/rt | **10**: 55[a]; 32[b] | 11[a] | None[a] |
| | | **11**: 34[a]; 18[b] | | |
| | 1 h/reflux | **10**: 58[a]; 35[b] | 15[a] | None[a] |
| | | **11**: 27[a]; 15[b] | | |

[a]Determined from $^1$H NMR spectra of the reaction crude.
[b]Isolated yield.

perturb the magnetic relaxation properties of water more effectively than the corresponding Gd-EDTA complexes.

The effects of Gd(III) complexes of compounds **1–4** on water relaxation are investigated in more detail in Table 2. This table summarizes the results of $T_1$ and $T_2$ measurements and corresponding longitudinal and transversal water relaxivities for the Gd(III) complexes of compounds **1–4**, EDTA and IDA. Heterocyclic complexones depicted higher $T_1$ relaxivity than IDA and slightly lower than EDTA. $T_2$ relaxivity increased in the order **1** < **2** < **3** < **4**, confirming the effects of these complexes on the water linewidth. Interestingly, transversal relaxivity of complexones **3** and **4** was twice that of EDTA. Taken together, these results indicate that Gd(III) complexes of compounds **3** and **4** may become useful contrast agents for MRI applications requiring $T_2$ weighting. This aspect is illustrated in Figure 2.

The figure shows a magnetic resonance image taken from a phantom consisting of three different capillaries containing saline, the Gd(III)-**4** complex and Gd(III)-EDTA complex, respectively. The left panel shows a proton density image in which the three capillaries depict similar intensity. The right panel shows a representative $T_2$-weighted image in which the capillary containing the complex Gd(III)-**4** appears as the darkest, confirming the stronger $T_2$ weighting effect than Gd(III)-EDTA.

### Themodynamic stability constants for Gd(III) and $Ca^{2+}$ complexation

Apparent stability constants for Gd(III) complexes from compounds **1–4**, EDTA and IDA were investigated spectrophotometrically by competition with the metallochromic indicator ArsenazoIII (ArsIII)[28] (Fig. 3). Titrations of ArsIII with Gd(III) depicted typical hyperbolic saturation curves, yielding an apparent stability constant of $2\times10^5$ M for the Gd(III)-ArsIII complex (0.15 M ionic strength, pH 6.7, 22 °C). For the same total amount of ArsIII and Gd(III) added, the presence of 10 mM IDA, 10 mM compounds **1–4** or 1 mM EDTA in the titration mixture caused a reduction in the amount of Gd(III) bound to ArsIII. This reduction reveals the

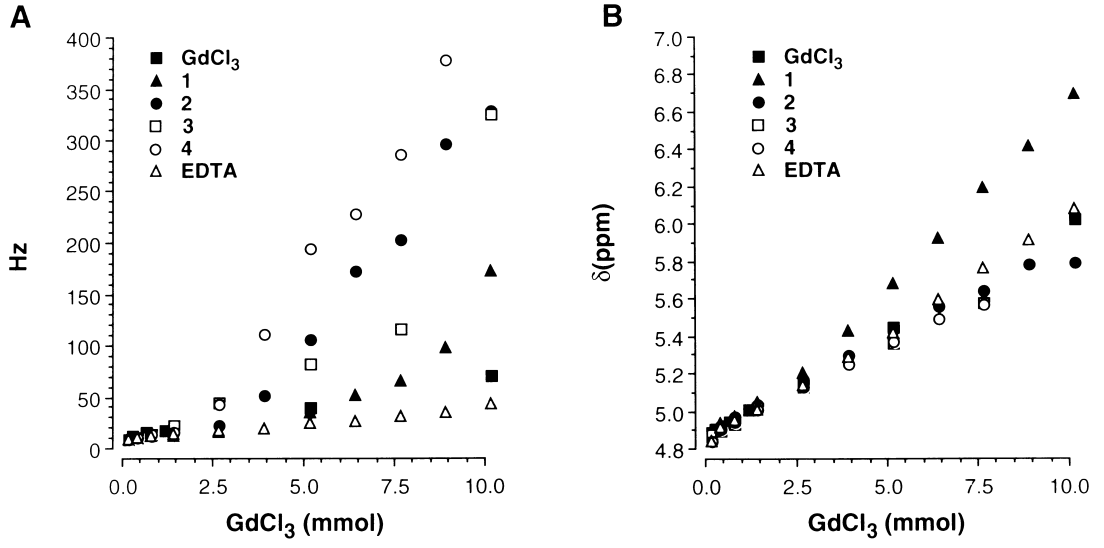


**Figure 1.** Effects of increasing Gd(III) concentrations on some magnetic properties of the water resonance in the presence and absence of complexones **1–4** or EDTA. $^1$H NMR spectra were acquired as indicated in Experimental. 25 mM compounds **1–4** or EDTA in $D_2O$ (99.9 D, pD 8–9, 22 °C, 1 mL final volume) were titered with $GdCl_3{\cdot}6H_2O$. A: Linewidth at half height. B: Chemical shift referred to external TSP.

**Table 2.** Inverse $T_1$ and $T_2$ values and longitudinal ($R_1$) and transverse ($R_2$) relaxivities of EDTA, IDA, and compounds **1–4**

| Compound | $\Delta\ 1/T_1$ | $R_1/M^{-1}s^{-1}$ | $\Delta\ 1/T_2$ | $R_2/M^{-1}s^{-1}$ |
|---|---|---|---|---|
| EDTA | 3.542 ± 0.037 | 7083 ± 145 (6) | 6.313 ± 0.232 | 12627 ± 590 (6) |
| IDA | 1.392 ± 0.036 | 2784 ± 99 (3) | 2.584 ± 0.273 | 5168 ± 597 (3) |
| **1** | 2.284 ± 0.033 | 4569 ± 112 (6) | 4.097 ± 0.289 | 8193 ± 660 (6) |
| **2** | 3.282 ± 0.123 | 6565 ± 312 (6) | 7.440 ± 0.567 | 14880 ± 1283 (12) |
| **3** | 2.885 ± 0.35 | 5770 ± 128 (6) | 11.651 ± 0.523 | 23302 ± 1278 (6) |
| **4** | 2.941 ± 0.031 | 5883 ± 121 (6) | 13.892 ± 1.511 | 27784 ± 3300 (12) |

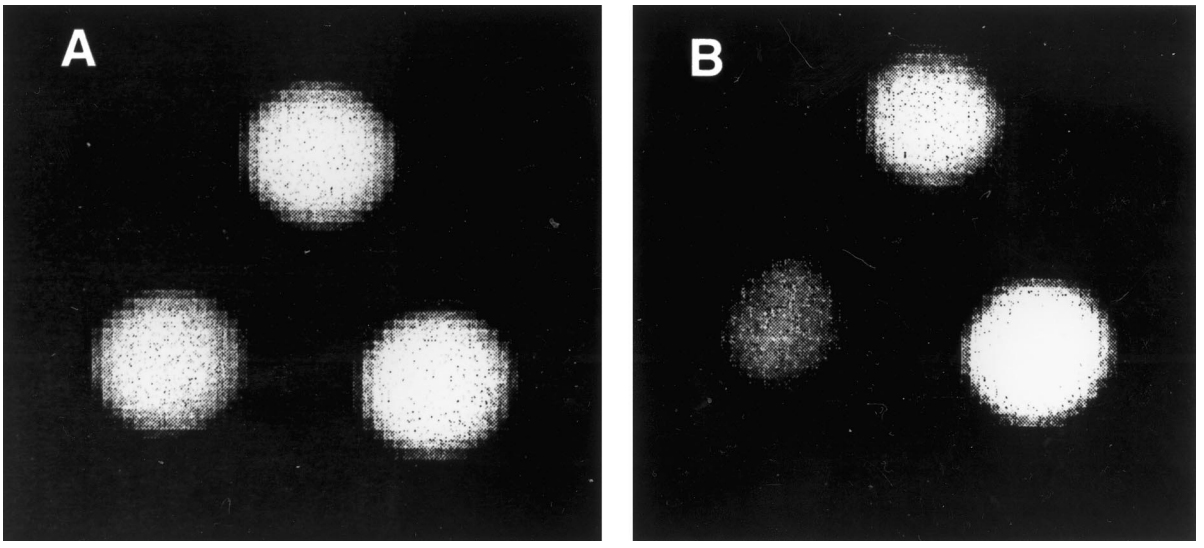


**Figure 2.** Spin echo MR images (360.1 MHz) of three capillaries (1 mm diameter) containing 0.5 mM Gd(III) and 1 mM EDTA in 155 mM NaCl (top), 0.5 mM Gd(III) and 10 mM compound **4** in 155 mM NaCl (bottom left) and 155 mM NaCl (bottom right). 100 mM Tris/HCl was used in all cases to buffer pH to 8.5. The three capillaries were placed in a 5 mm $^1$H NMR tube. MR images were acquired as indicated in Experimental. (A) Proton density image, TR: 15 s, TE: 2 ms. (B) $T_2$ weighted image, TR: 15 s, TE: 43 ms. Slice thickness: 1 mm. Pixel size: 78 μ×78 μ.

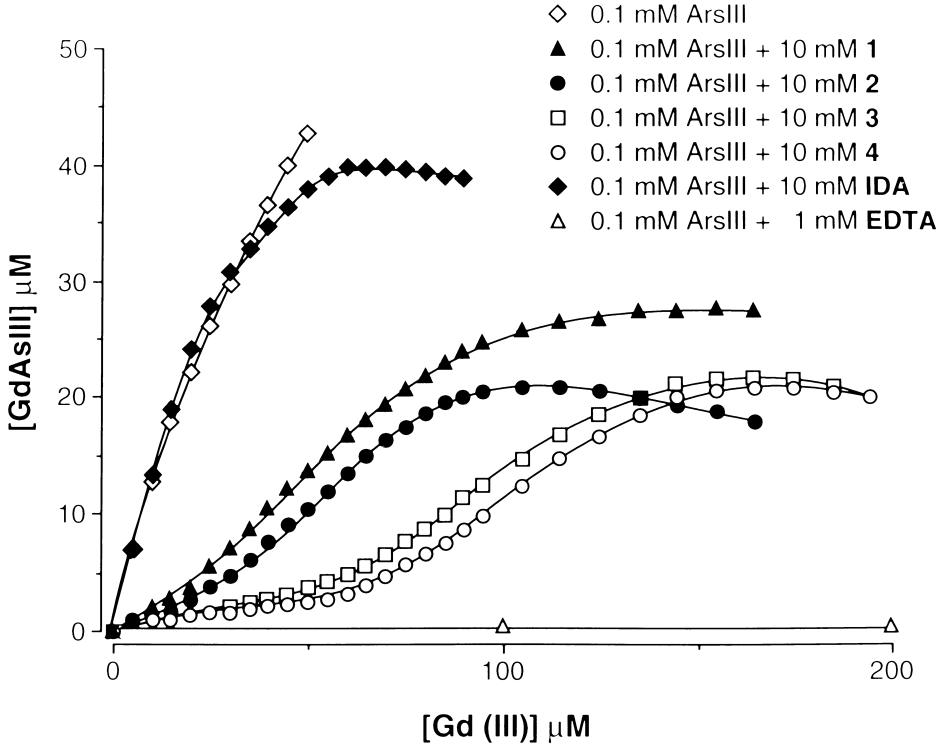


**Figure 3.** Titrations (25 °C, pH 6.7, 0.1 M $NH_4Cl$) of ArsIII (0.1 mM) with Gd(III) in the absence and presence of compounds **1–4** (10 mM), EDTA (1 mM), or IDA (10 mM). The concentration of the Gd(III)-ArsIII complex (GdAs) was measured spectrophotometrically as indicated in Experimental. The symbols refer to titrations of the different complexones. Continuous lines show the results of simulations performed with optimized values of the corresponding stability constants (K′).

amount of Gd(III) bound to the complexone and permits calculation of the stability constant of the Gd(III) complexone complex. Different titration behavior was observed in IDA, EDTA and complexones **1–4**. EDTA presented a much higher affinity constant for Gd(III) than ArsIII causing no ArsIII-Gd(III) complex formation when the concentration of EDTA was higher than ArsIII. In contrast, the IDA titration curve was similar to that of ArsIII revealing no significant competition for Gd(III) between these two ligands. Complexones **3** and **4** showed an intermediate behavior between IDA and EDTA. In these cases, a sigmoidal binding pattern appeared, revealing the presence of two different binding modes. At low concentrations of Gd(III), complexones

**3** and **4** depicted a similar affinity for Gd(III) than EDTA and only a small amount of Gd(III)-ArsIII complex was formed. However, at concentrations of Gd(III) higher than 50 μM, a lower affinity binding mode similar to that of IDA appeared in the complexones, as revealed by the increased concentration of Gd(III)-ArsIII complex. The high affinity binding mode most probably represents a tetradentate coordination chelate of complexones **1–4**, similar to the pentadentate Gd(III)-EDTA complex at pH 7.0. The low affinity binding mode represents most probably a tridentate complex similar to that of Gd(III)-IDA. Thus, complexones **1–4** present different Gd(III) binding properties depending on the relative concentrations of Gd(III) to complexone. Computer simulations permitted the estimation of values for the stability constants (K′) of the different complexes formed. Optimal simulations of the titration curves were obtained when values for the stability constants of the high affinity binding modes of **1** and **4** were $10^5$ M, a very similar value to that obtained for EDTA at the same pH ($10^6$ M). Similarly, simulations of binding isotherms revealed values for the low affinity binding modes of: IDA = 26.1 M; **1** = 48.8 M; **2** = 60.6 M; **3** = 40.8 M; **4** = 40.0 M.

Additionally, stability constants for $Ca^{2+}$ of compounds **1–4**, IDA and EDTA were determined potentiometrically with a $Ca^{2+}$ selective electrode. Log K′ values were (pH 9.0); **1** (3.35), **2** (2.77), **3** (3.75), **4** (3.04), IDA (2.24), EDTA (7.12). Thus, compounds **1–4** and IDA present similar $Ca^{2+}$ binding properties revealing that the azole moiety is not effectively involved in $Ca^{2+}$ complexation.

## Calculations of molecular geometry

We performed semiempirical (PM3) calculations of the structure of chelates from compounds **1–4**, EDTA, and IDA with three different cations: $Ca^{2+}$, $Mg^{2+}$, and Gd(III). The geometry of the complex is determined by the cation, originating in all cases a cage structure in which the cation is buried. Calculated bond orders and effective charges on the metal for **1–4**, IDA, and EDTA are given in Table 3. Figure 4 depicts an illustrative example of the optimized geometries from the Gd(III) complexes of compounds **3** (panel A) and **4** (panel B). Low values of metal effective charge and high values of metal bond orders infer high affinity for the metal. Taking into account the bond order and the effective charge on the cation, the following metal chelation capacities can be deduced from the calculations: $Mg^{2+}$: IDA < **1** = **2** = **3** = **4** < EDTA; $Ca^{2+}$: IDA < **1** = **2** = **3** = **4** < EDTA; Gd(III): IDA < **1** = **2** = EDTA < **3** = **4**. Notably, these calculated results matched well with the stability constants determined experimentally for $Ca^{2+}$ and Gd(III).

The participation of the azole ring in the complexation was comfirmed experimentally. $^1$H NMR spectra of compounds **3** and **4** obtained with increasing Gd(III) concentrations showed that protons from the azole moiety and the iminodiacetic part were shifted similarly by the paramagnetic ion. Indeed, the lanthanide induced shifts (LIS) in these compounds were similar to those obtained in EDTA. Since the magnitude of LIS values is related to the distance of a proton to the paramagnetic center,[29] these results confirm that the azole moiety is involved in the complexation as indicated by the theoretical calculations. In contrast, shifts induced in $Ca^{2+}$ titrations in the protons from the azole moiety were negligible.

**Table 3.** Heat of formation ($H_f$, kcal/mol), effective charges (e), and bond orders of calculated geometries of complexes from compounds **1–4**, EDTA, and IDA with $Mg^{2+}$, $Ca^{2+}$, and Gd(III)

| Complex | $H_f$ | Metal effective charge[a] | Metal bond order |
|---|---|---|---|
| **1**-Mg | −187 | 0.9 | 2.6 |
| **2**-Mg | −193 | 0.9 | 2.6 |
| **3**-Mg | −162 | 0.8 | 2.6 |
| **4**-Mg | −151 | 0.9 | 2.6 |
| IDA-Mg | −234 | 1.2 | 2.3 |
| EDTA-Mg | −449 | 0.7 | 2.7 |
| **1**-Ca | −292 | 2.5 | 1.5 |
| **2**-Ca | −325 | 2.5 | 1.5 |
| **3**-Ca | −295 | 2.5 | 1.5 |
| **4**-Ca | −288 | 2.5 | 1.5 |
| IDA-Ca | −-286 | 3.0 | 1.2 |
| EDTA-Ca | −607 | 2.3 | 1.6 |
| **1**-Gd | −220 | 2.5 | 3.2 |
| **2**-Gd | −247 | 2.5 | 3.2 |
| **3**-Gd | −227 | 2.4 | 3.3 |
| **4**-Gd | −215 | 2.5 | 3.2 |
| IDA-Gd | −182 | 3.1 | 2.7 |
| EDTA-Gd | −699 | 2.6 | 3.2 |

[a]Metal effective charge = Mulliken charge + electrostatic charge.

## Toxicity assays

Figure 5 shows the results of toxicity tests performed with cultures of H35 hepatoma cells. Compounds **1–4**, IDA, and EDTA were added to the cultures in increasing concentrations of 10 μM, 100 μM, and 1 mM in the absence and presence of Gd(III). Toxicity was assayed as the release of LDH to the medium after incubations of the cells with the complexones for increasing periods of time up to 6 h. In the absence of Gd(III) all compounds had similar toxicity with the exception of **1**. In the presence of Gd(III), the toxicity of compounds **2–4** was not increased.

## Discussion

Although the physical theories of relaxivity in complexes of paramagnetic ions used as contrast agents in MRI are considerably developed, less is known on the relation between chemical structure of the ligand and relaxivity. The present study provides a useful frame to address this topic. Measurements of relaxation times indicate that heterocyclic complexones **3** and **4** originate paramagnetic Gd(III)-complexes with significantly improved $T_2$ relaxivity compared with the more classical complexones like EDTA, DTPA, or DOTA, which do not contain heterocycles.[4] This is a remarkable finding since the classical Gd(III) complexes are known as $T_1$ relaxivity enhancers.

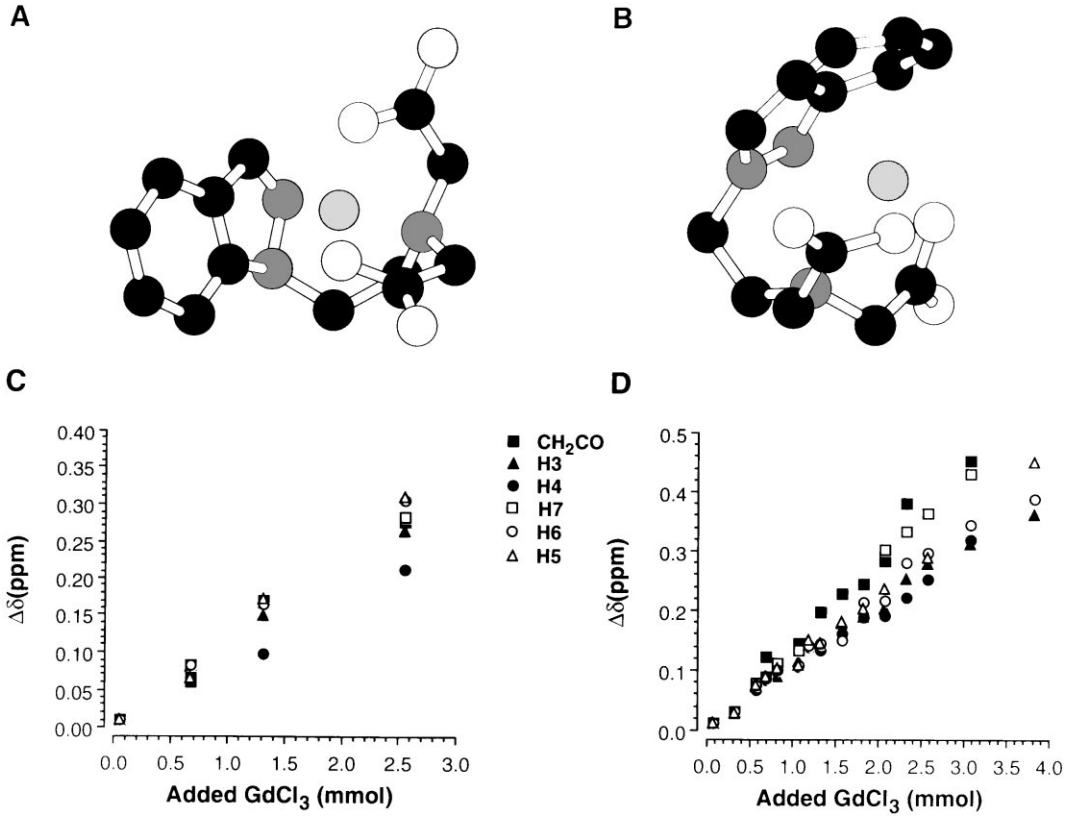


**Figure 4.** Semiempirical PM3 calculations of the optimized geometries of Gd(III) complexes from compounds **3** (A) and **4** (B). Effect of increasing Gd(III) concentrations on the chemical shifts of the protons from compounds **3** (C) and **4** (D). Titrations were performed as in Figure 1. Δδ indicates downfield shift induced by Gd(III).

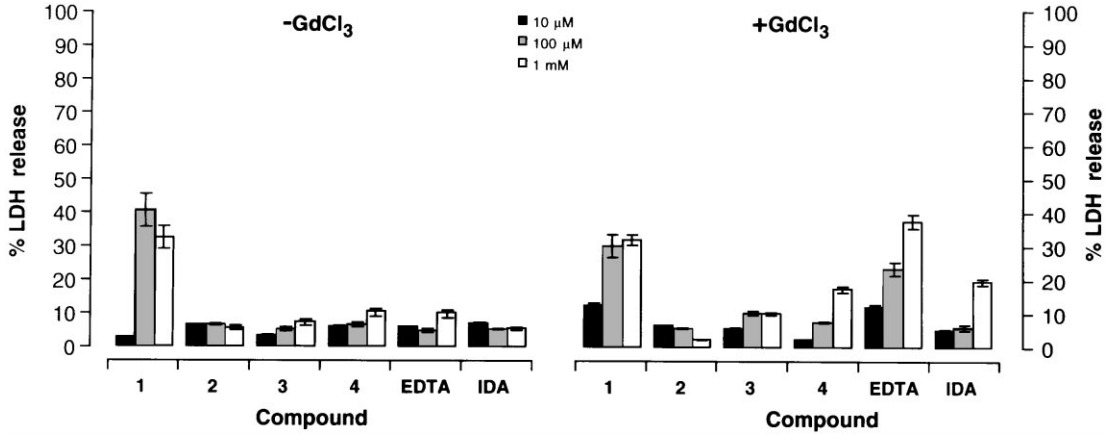


**Figure 5.** Toxicity assays of compounds **1–4**, IDA, and EDTA in the absence (left) and presence (right) of Gd(III). Acute toxicity was determined in vitro measuring the release of LDH to the medium in cultures of H35 cells incubated for 1 h with increasing concentrations of the compounds. LDH release is expresed as a percentage of total releasable LDH. When present, Gd(III) was added as 10% of the total concentration of compounds **1–4** and IDA or equimolar concentration of EDTA.

$T_1$ or $T_2$ relaxivity in paramagnetic complexes is thought to depend on the electronic charge distribution around the paramagnetic ion.[30] $T_1$ relaxivity enhancement in Gd(III) complexes was proposed to depend on the isotropic charge distribution around Gd(III). In contrast, improved $T_2$ relaxivity in paramagnetic complexes of EDTA, DTPA or DOTA could be obtained only when Gd(III) was substituted by other lanthanides with an unsymmetrical charge distribution such as Dy(III).[31] The present study shows that $T_2$ relaxivity can also be induced in Gd(III) complexes when an appropriate unsymmetrical ligand is used. The substitution in **3** and **4** of one iminodiacetic moiety of EDTA by a benzazole ring results in an unsymmetrical structure containing four chemically different donor sites: two carboxylic groups and a tertiary amino group from the iminodiacetic part and the benzazole. MO calculations support these interpretations showing that the species containing the azole ring as donor, folds over creating an unsymmetrical cavity in which the metal is placed

(Fig. 4). Cage structures are typical of many chelates and a symmetrical cage structure has been resolved by X-ray diffraction of several Ln(III)-EDTA chelates.[32]

Relaxivity effects are the consequence of additive inner sphere and outer sphere effects. These effects involve magnetic relaxation of the water molecules in direct contact with the paramagnetic ion and of those water molecules further away in the solution, respectively.[30] It is possible to analyze the $T_1$ or $T_2$ relaxivity effects in complexones **3** and **4** in terms of these inner or outer sphere contributions. Expressions describing the inner sphere effects on $T_1$ and $T_2$ relaxivity are:

$$\frac{1}{T_{1is}} = \frac{[C]q}{55.6} \frac{1}{T_{1M} + \tau_M}$$

$$\frac{1}{T_{2is}} = \frac{[C]q}{55.6} (\delta\omega)^2 \tau_M$$

where [C] is the molar concentration of paramagnetic ion, q the number of water ligands per ion, $T_{1M}$ is the longitudinal relaxation time of water protons bound to the metal ion and in rapid exchange with the solvent, $\tau_M$ is the residence time of these water molecules in the complex and $\delta\omega$ is the chemical shift effect.[30] Thus, inner sphere $T_1$ and $T_2$ relaxivities depend on the number of water molecules in direct contact with the ion and their residence time, but $T_2$ relaxivity depends additionally on a chemical shift effect. In contrast, theory indicates that outer sphere contributions to $T_1$ and $T_2$ relaxivity do not depend on the number of water molecules coordinated to the metal ion or on the chemical shift effects.[30] For a nine or 10 possible coordination sites in free Gd(III), high affinity binding modes of the Gd(III) complexes of **3** and **4** form tetradentate complexes (Fig. 4), leaving up to five or six coordination sites for water in the first coordination sphere. This number of water molecules is larger than the three water molecules bound to Gd(III)-EDTA complex or the single water molecule bound to the Gd(III)-DTPA complex. Thus, increased $T_2$ relaxivity in Gd(III) complexes of **3** and **4** appears to be caused mainly by an inner sphere effect due to the increased number of water molecules in the first coordination sphere of the Gd(III). We propose that hydrogens from the various water molecules experience different deshilding effects. Thus, the resulting chemical shifts vary for every water molecule depending from the balance of the electronic contributions of metal and ligand. These ligand induced shifts are anysotropic due to the different location of the azole moiety and the iminodiacetic acid part in the complex, affecting the $(\delta\omega)^2$ term and therefore $T_2$.

## Conclusions

We have synthesized a novel series of complexones containing azole rings, *N*-2-(azol-1(2)-yl)ethyliminodiacetic acids. The new complexones show improved $T_2$ relaxivity than Gd(III) complexes of EDTA. This is an interesting finding since previous Gd(III) complexes were considered mainly as $T_1$ enhancers. $^1$H NMR measurements in solution combined with MO calculations indicate that the structure of these complexes is governed by the metal, giving cage structures where the paramagnetic ion is inserted. The toxicity in vitro of the Gd(III) complexes of these heterocyclic complexones is lower than that of Gd(III)-EDTA.

## Experimental

### General

Melting points were obtained on a microscope hot stage and are uncorrected. Elemental analyses were performed with a Perkin–Elmer 240 apparatus. Mass spectra were carried out (GC/mass spectrometer Schimadzu QP-5000) at 70 eV. IR spectra were determined on a Philips PU-9700 spectrophotometer. NMR spectra were recorded with a Bruker AC-200 (200.13 MHz for $^1$H, and 50.33 MHz for $^{13}$C). $^1$H and $^{13}$C chemical shifts ($\delta$) in $CDCl_3$ are given from internal tetramethylsilane, $^1$H $\delta$ in $D_2O$ are given from external 3-trimethylsilyl(tetradeutero)propionic acid sodium salt, and $^{13}$C $\delta$ in $D_2O$ are given from external DMSO-$d_6$, with an accuracy of $\pm 0.01$ for $^1$H and $\pm 0.1$ ppm for $^{13}$C. The residual water signal in $^1$H NMR spectra in $D_2O$ solutions was suppressed when necessary using a 1 s (low power, 0.5 watts) presaturating pulse applied with the decoupler. $^1$H–$^1$H coupling constants ($J$) are accurate to $\pm 0.2$ Hz for $^1$H NMR spectra. TLC chromatography was performed on DC-Alufolien/Kieselgel 60 $F_{254}$ (Merck, 0.2 mm) and column chromatography through silica gel Merck 60 (70–230 mesh). Methyl iminodiacetate hydrochloride was obtained from iminodiacetodinitrile,[26] and basified with solid $Na_2CO_3$ in the minimum amount of water prior to use. $D_2O$ (99.9 D) was purchased from Appollo Scientific (Stockport, Great Britain). The rest of the products were purchased from Aldrich.

**Synthesis of 1(2)-(2-bromoethyl)azoles. General method.** A one-necked round-bottomed flask was fitted with a reflux condenser and with a magnetic stirrer. The flask was charged with 40% NaOH, the azole, tetrabutylammonium bromide (TBAB), and 1,2-dibromoethane (3:1:1/40:10 molar ratio). The reaction mixture was left to stir under the conditions shown in Table 1. The organic phase was then separated, dried and evaporated in vacuo. The residue was purified by column chromatography and/or distillation.

**1-(2-Bromoethyl)pyrazole (8).** (From 29.4 to 117.6 mmol of azole). $bp_{0.01}$ 38–40 °C. IR (film): 3110, 3020, 2970, 2920, 1510, 1445, 1410, 1395, 1290, 1260, 1215, 1125, 1090, 1050, 965, 915, 880, 755 cm$^{-1}$. MS: $m/z$ 176 (M + 1, 11%), 174 (M − 1, 11%), 95 (31%), 81 (41%), 69 (8%), 68 (100%), 54 (15%), 53 (17%), 52 (8%). $^1$H NMR ($CDCl_3$, $\delta$):[23] 7.56 (d, 1H, $^3J_{34} = 1.6$ Hz, H3), 7.46 (d, 1H, $^3J_{45} = 2.1$ Hz, H5), 6.26 (apparent triplet, 1H, H4), 4.51 (t, 2H, $^3J = 6.4$ Hz, C$H_2$-N), 3.72 (t, 2H, $^3J = 6.4$ Hz, C$H_2$-Br); $^{13}$C NMR ($CDCl_3$, $\delta$): 139.8 (d, $^1J_{C3H3} = 185.2$ Hz, C3), 129.7 (d, $^1J_{C5H5} = 186.4$ Hz, C5),

105.1 (d, $^1J_{C4H4}$ = 177.0 Hz, C4), 52.9 (t, $^1J$ = 141.6 Hz, $CH_2$-N), 30.2 (t, $^1J$ = 153.6 Hz, $CH_2$-Br).

**1-(2-Bromoethyl)-3,5-dimethylpyrazole (9).** (For 14.0 mmol of azole). Chromatographic eluent: ethyl acetate. $bp_{0.05}$: 46–48 °C Lit.[24] $bp_{0.4}$ 89–90 °C. IR (film): 3130, 3030, 2960, 2920, 2870, 1550, 1455, 1420, 1385, 1300, 1260, 1215, 1145, 1030, 975, 880, 780 $cm^{-1}$. MS: *m/z* 204 (M + 1, 11%), 203 (M, 1%), 202 (M−1, 11%), 123 (4%), 109 (43%), 97 (6%), 96 (100%), 95 (35%), 82 (6%), 81 (6%), 68 (11%), 55 (6%). $^1$H NMR ($CDCl_3$, δ): 5.79 (s, 1H, H4), 4.31 (t, 2H, $^3J$ = 6.7 Hz, C$H_2$-N), 3.68 (t, 2H, $^3J$ = 6.7 Hz, C$H_2$-Br), 2.27 (s, 3H, C$H_3$-5-), 2.21 (s, 2 H, C$H_3$-3-); $^{13}$C NMR ($CDCl_3$, δ): 148.0 (s, C3), 139.2 (s, C5), 104.9 (d, $^1J_{C4H4}$ = 172.6 Hz, C4), 49.3 (t, $^1J$ = 140.7 Hz, C$H_2$-N), 30.2 (t, $^1J$ = 153.4 Hz, C$H_2$-Br), 13.3 (q, $^1J$ = 126.9 Hz, C$H_3$-3-), 10.8 (q, $^1J$ = 128.5 Hz, $CH_3$-5-).

**1-(2-Bromoethyl)indazole (10).** (From 4.24 to 17.0 mmol of azole). Chromatographic eluent: hexane:ethyl acetate, 6:4. IR (film): 3080, 3060, 2980, 2940, 1645, 1615, 1500, 1465, 1435, 1420, 1315, 1300, 1275, 1230, 1210, 1160, 1010, 910, 850, 835, 755, 745 $cm^{-1}$. MS: *m/z* 226 (M + 1, 17%), 225 (M, 1%), 224 (M−1, 17%), 132 (9%), 131 (100%), 118 (16%), 104 (11%), 103 (15%), 89 (8%), 77 (21%), 63 (17%), 51 (9%). $^1$H NMR ($CDCl_3$, δ): 8.04 (d, 1H, $^5J_{37}$ = 0.8 Hz, H3), 7.78 (ddd, 1H, $^3J_{45}$ = 8.0 Hz, $^4J_{46}$ = 0.9 Hz, $^5J_{47}$ = 0.9 Hz, H4), 7.53–7.38 (m, 2H, H6 y H7), 7.20 (ddd, 1H, $^3J_{45}$ = 8.0 Hz, $^3J_{56}$ = 6.2 Hz, $^4J_{57}$ = 1.8 Hz, H5), 4.76 (t, 2H, $^3J$ = 6.8 Hz, C$H_2$-N), 3.79 (t, 2H, $^3J$ = 6.8 Hz, C$H_2$-Br); $^{13}$C NMR ($CDCl_3$, δ): 139.5 (s, C7a), 133.7 (d, $^1J_{C3H3}$ = 189.9 Hz, C3), 126.3 (d, $^1J_{C6H6}$ = 165.7 Hz, C6), 123.6 (s, C3a), 120.9 (d, $^1J_{C5H5}$ = 154.9 Hz, C5), 120.6 (d, $^1J_{C4H4}$ = 165.4 Hz, C4), 49.7 (t, $^1J$ = 141.4 Hz, $CH_2$-N), 29.4 (t, $^1J$ = 153.5 Hz, $CH_2$-Br).

**2-(2-Bromoethyl)indazole (11).** (From 4.24 to 17.0 mmol of azole). Chromatographic eluent: hexane:ethyl acetate, 6:4. IR (film): 3120, 3060, 2970, 2920, 1625, 1510, 1470, 1425, 1380, 1350, 1310, 1265, 1160, 1140, 785, 760 $cm^{-1}$. MS: *m/z*: 226 (M + 1, 11%), 225 (M, 1%), 224 (M−1, 11%), 119 (9%), 118 (100%), 103 (4%), 91 (9%), 89 (9%), 77 (10%), 63 (16%), 51 (5%). $^1$H NMR ($CDCl_3$, δ): 8.00 (d, 1H, $^5J_{37}$ = 0.8 Hz, H3), 7.70 (dddd, 1H, $^3J_{67}$ = 7.3 Hz, $^4J_{57}$ = 0.9 Hz, $^5J_{47}$ = 1.0 Hz, $^5J_{37}$ = 0.8 Hz, H7), 7.66 (ddd, 1H, $^3J_{45}$ = 7.3 Hz, $^4J_{46}$ = 1.0 Hz, $^5J_{47}$ = 1.0 Hz; H4), 7.30 (ddd, 1H, $^3J_{67}$ = 7.3 Hz, $^3J_{56}$ = 6.7 Hz, $^4J_{46}$ = 1.0 Hz, H6), 7.10 (ddd, 1H, $^3J_{45}$ = 7.3 Hz, $^3J_{56}$ = 6.7 Hz, $^4J_{57}$ = 0.9 Hz, H5), 4.76 (t, 2H, $^3J$ = 6.3 Hz, C$H_2$-N), 3.79 (t, 2H, $^3J$ = 6.3 Hz, C$H_2$-Br); $^{13}$C NMR ($CDCl_3$, δ): 149.0 (s, C7a), 126.1 (d, $^1J_{C6H6}$ = 160.6 Hz, C6), 123.6 (d, $^1J_{C3H3}$ = 189.9 Hz, C3), 121.6 (d, $^1J_{C5H5}$ = 159.7 Hz, C5), 121.2 (s, C3a), 120.1 (d, $^1J_{C4H4}$ = 156.4 Hz, C4), 117.0 (d, $^1J_{C7H7}$ = 167.0 Hz, C7), 54.5 (t, $^1J$ = 142.6 Hz, C$H_2$-N), 29.4 (t, $^1J$ = 155.6 Hz, $CH_2$-Br).

**Synthesis of methyl *N*-2-(azol-1(2)-yl)ethyliminodiacetates. General procedure.** A 1-necked round-bottomed flask was fitted with a reflux condenser attached to a drying tube ($CaCl_2$) and with a magnetic stirrer. The flask was charged with the corresponding bromoethylazole and methyl iminodiacetate (1:2 molar ratio). The mixture was heated with stirring in an oil bath at 110 °C for 2.5 to 4.5 h. After cooling at room temperature the mixture was extracted with $CH_2Cl_2$. Organic solvent was evaporated in vacuo and the residue purified by column chromatography and/or distillation.

**Methyl *N*-(2-pyrazol-1-yl)ethyliminodiacetate (12).** (From 2.24 to 6.7 mmol of 1-(2-bromoethyl)pyrazole). Reaction time: 2.5 h. Chromatographic eluent: hexane:ethanol, 8:2. $bp_{0.01}$ 128–130 °C. Yield: 55%. IR (film): 3140, 3120, 3000, 2960, 2840, 1740, 1510, 1435, 1395, 1365, 1280, 1205, 1180, 1145, 1090, 1060, 1040, 1010, 880, 760 $cm^{-1}$. MS: *m/z*: 256 (M + 1, 4%), 255 (M, 13%), 196 (28%), 188 (6%), 187 (50%), 174 (55%), 146 (40%), 128 (70%), 116 (27%), 100 (17%), 95 (17%), 94 (14%), 81 (18%), 69 (14%), 68 (37%), 59 (18%), 56 (25%), 54 (18%), 45 (100%). $^1$H NMR ($CDCl_3$, δ): 7.53 (d, 1H, $^3J_{34}$ = 1.8 Hz, H3), 7.50 (d, 1H, $^3J_{45}$ = 2.0 Hz, H5), 6.22 (apparent triplet, 1H, H4), 4.24 (t, 2H, $^3J$ = 6.2 Hz, C$H_2$-Azole), 3.19 (t, 2H, $^3J$ = 6.2 Hz, C$H_2$-N-); $^{13}$C NMR ($CDCl_3$, δ): 171.6 (s, 2C, CO), 139.3 (d, $^1J_{C3H3}$ = 186.9 Hz, C3), 130.0 (d, $^1J_{C5H5}$ = 190.9 Hz, C5), 105.1 (d, $^1J_{C4H4}$ = 176.3 Hz, C4), 55.3 (t, 2C, $^1J$ = 136.5 Hz, *C*$H_2$-CO-), 54.7 (t, $^1J$ = 135.8 Hz, $CH_2$-N-), 51.5 (q, 2C, $^1J$ = 147.2 Hz, $CH_3$), 51.2 (t, $^1J$ = 139.6 Hz, $CH_2$-Azole). Picrate: mp 91–93 °C. Anal. calcd for $C_{17}H_{20}N_6O_{11}$: C, 42.34; H, 4.07; N, 17.08. Found: C, 42.31; H, 4.10; N, 17.11.

**Methyl *N*-2-(3,5-dimethylpyrazol-1-yl)ethyliminodiacetate (13).** (From 2.46 to 5.55 mmol of 1-(2-bromoethyl)-3,5-dimethylpyrazole). Reaction time: 3.5 h. $bp_{0.01}$ 140–142 °C. Yield: 65%. IR (Film): 3130, 3000, 2960, 2930, 2870, 2220, 1740, 1550, 1435, 1385, 1260, 1200, 1180, 1170, 1120, 1050, 1020, 915, 775, 730 $cm^{-1}$. MS: *m/z*: 283 (M, 5%), 224 (13%), 187 (28%), 174 (27%), 146 (35%), 128 (55%), 124 (7%), 116 (19%), 114 (6%), 109 (7%), 100 (9%), 97 (19%), 96 (16%), 82 (14%), 68 (6%), 59 (9%), 56 (12%), 54 (7%), 45 (100%). $^1$H NMR ($CDCl_3$, δ): 5.74 (s, 1H, H4), 4.07 (t, 2H, $^3J$ = 6.8 Hz, C$H_2$-Azole), 3.67 (s, 6H, C$H_3$), 3.47 (s, 4H, C$H_2$-CO-), 3.09 (t, 2H, $^3J$ = 6.8 Hz, C$H_2$-N-), 2.24 (s, 3H, C$H_3$-5-), 2.18 (s, 3H, $CH_3$-3); $^{13}$C NMR ($CDCl_3$, δ): 171.2 (s, 2C, *C*O), 147.0 (s, C3), 139.1 (s, C5), 104.4 (d, $^1J_{C4H4}$ = 172.1 Hz, C4), 55.1 (t, 2C, $^1J$ = 136.4 Hz, $CH_2$-CO-), 54.2 (t, $^1J$ = 136.6 Hz, $CH_2$-N-), 51.1 (q, 2C, $^1J$ = 142.1 Hz, $CH_3$), 47.5 (t, $^1J$ = 138.8 Hz, $CH_2$-Azole), 13.0 (q, $^1J$ = 123.4 Hz, $CH_3$-3-), 10.5 (q, $^1J$ = 127.9 Hz, $CH_3$-5-). Picrate: mp: 83–85 °C. Anal. calcd for $C_{19}H_{24}N_6O_{11}$: C, 44.53; H, 4.69; N, 16.41. Found: C, 44.58; H, 4.64; N, 16.54.

**Methyl *N*-2-(indazol-1-yl)ethyliminodiacetate (14).** (For 6 mmol of 1-(2-bromoethyl)indazole). Reaction time: 4.5 h. $bp_{0.01}$ 160–162 °C. Yield: 56%. IR (film): 3060, 3000, 2950, 2850, 1740, 1610, 1505, 1470, 1435, 1315, 1200, 1180, 1160, 1120, 1085, 1010, 910, 830, 755, 740 $cm^{-1}$. MS: *m/z*: 305 (M, 6%), 246 (11%), 187 (23%), 175 (6%), 174 (72%), 146 (39%), 131 (6%), 128 (17%), 118 (11%), 116 (20%), 115 (6%), 94 (10%), 91 (5%), 77 (14%), 56 (8%), 51 (5%), 45 (100%). $^1$H NMR ($CDCl_3$, δ): 7.99 (d, $^1$H, $^5J_{37}$ = 0.8 Hz, H3), 7.71

(ddd, 1H, $^3J_{45}=8.1$ Hz, $^4J_{46}=1.0$ Hz, $^5J_{47}=1.0$ Hz, H4), 7.50 (dddd, 1H, $^3J_{67}=8.1$ Hz, $^4J_{57}=0.8$ Hz, $^5J_{47}=1.0$ Hz, $^5J_{37}=0.8$ Hz, H7), 7.37 (ddd, 1H, $^3J_{67}=8.1$ Hz, $^3J_{56}=6.8$ Hz, $^4J_{46}=1.0$ Hz, H6), 7.13 (ddd, 1H, $^3J_{45}=8.1$ Hz, $^3J_{56}=6.8$ Hz, $^4J_{57}=0.8$ Hz, H5) 4.54 (t, 2H, $^3J=6.8$ Hz, C$H_2$-azole), 3.65 (s, 6H, C$H_3$), 3.49 (s, 4H, CO-C$H_2$-N), 3.26 (t, 2H, $^3J=6.8$ Hz, C$H_2$-N-); $^{13}$C NMR ($CDCl_3$, δ): 171.1 (s, 2C, *C*O), 139.4 (s, C7a), 132.7 (d, $^1J_{C3H3}=189.3$ Hz, C3), 125.8 (d, $^1J_{C6H6}=160.7$ Hz, C6), 123.6 (s, C3a), 120.5 (d, $^1J_{C5H5}=161.3$ Hz, C5), 120.1 (d, $^1J_{C4H4}=160.9$ Hz, C4), 108.9 (d, $^1J_{C7H7}=163.6$ Hz, C7), 55.1 (t, 2C, $^1J=137.8$ Hz, *C*$H_2$-CO-), 53.5 (t, $^1J=135.8$ Hz, $CH_2$-N-), 51.1 (q, 2C, $^1J=147.0$ Hz, $CH_3$), 47.7 (t, $^1J=139.2$ Hz, $CH_2$-azole). Picrate: mp 105.5–107.5 °C. Anal. calcd for $C_{21}H_{22}N_6O_{11}$: C, 47.19; H, 4.20; N, 15.73. Found: C, 46.80; H, 4.07; N, 15.31.

**Methyl *N*-2-(indazol-2-yl)ethyliminodiacetate (15).** (For 3.32 mmol of 2-(2-bromoethyl)indazole). Kugelrorh $ot_{0.01}$: 250 °C. Yield: 60%. IR (film): 3120, 3060, 3000, 2960, 1735, 1620, 1505, 1430, 1375, 1355, 1200, 1180, 1160, 1055, 1010, 980, 905, 785, 760, 745 $cm^{-1}$. MS: *m*/*z*: 305 (M, 10%), 246 (11%), 187 (31%), 174 (26%), 146 (28%), 128 (57%), 119 (8%), 118 (36%), 116 (13%), 114 (10%), 100 (9%), 94 (6%), 91 (6%), 89 (6%), 77 (9%), 59 (10%), 56 (7%), 54 (5%), 45 (100%). $^1$H NMR ($CDCl_3$, δ): 8.11 (d, 1H, $^5J_{37}=0.9$ Hz, H3), 7.69 (dddd, 1H, $^3J_{67}=7.7$ Hz, $^4J_{57}=1.0$ Hz, $^5J_{47}=1.2$ Hz, $^5J_{37}=0.9$ Hz, H7), 7.65 (ddd, 1H, $^3J_{45}=6.3$ Hz, $^4J_{46}=1.2$ Hz, $^5J_{47}=1.2$ Hz, H4) 7.27 (ddd, 1H, $^3J_{56}=8.3$ Hz; $^3J_{67}=7.7$ Hz, $^4J_{46}=1.2$ Hz, H6), 7.06 (ddd, 1H, $^3J_{56}=8.3$ Hz, $^3J_{45}=6.3$ Hz, $^4J_{57}=1.0$ Hz, H5), 4.52 (t, 2H, $^3J=6.1$ Hz, C$H_2$-azole), 3.65 (s, 6H, C$H_3$), 3.46 (s, 4H, C$H_2$-CO-), 3.35 (t, 2H, $^3J=6.1$ Hz, C$H_2$-N-); $^{13}$C NMR ($CDCl_3$, δ): 171.5 (s, 2C, CO), 148.7 (s, C7a), 125.7 (d, $^1J_{C6H6}=165.2$ Hz, C6), 124.0 (d, $^1J_{C3H3}=190.3$ Hz, C3), 121.5 (s, C3a), 121.2 (d, $^1J_{C4H4}=159.4$ Hz, C4), 120.1 (d, $^1J_{C5H5}=165.2$ Hz, C5), 117.0 (d, $^1J_{C7H7}=160$ Hz, C7), 55.5 (t, 2C, $^1J=137.6$ Hz, $CH_2$-CO-), 55.0 (t, $^1J=136.5$ Hz, $CH_2$-N-), 52.7 (t, $^1J=141.2$ Hz, $CH_2$-azole), 51.4 (q, 2C, $^1J=147.2$ Hz, *C*$H_3$). Picrate: mp 141–142 °C. Anal. calcd for $C_{21}H_{22}N_6O_{11}$: C, 47.19; H, 4.20; N, 15.73. Found: C, 47.40; H, 4.62; N, 15.61.

***N*-(2-Pyrazol-1-yl)ethyliminodiacetic acid hydrochloride (16).** A 1-necked round-bottomed flask was fitted with a reflux condenser and with a magnetic stirrer. The flask was charged with compound **12** (0.7 mmol) and 2 N HCl (1:18 molar ratio). The solution was heated in an oil bath at 100 °C for 4 h. After cooling at room temperature the solvent was removed in vacuo and the residue dried over $P_2O_5$ in vacuo. Compound **12** was recrystallized from ethanol:diethyl ether. mp 142.5–144.5 °C. $^1$H NMR ($D_2O$, δ): 7.70 (d, 1H, $^3J_{45}=2.4$ Hz, H5), 7.61 (d, 1H, $^3J_{34}=2.2$ Hz, H3), 6.31 (apparent triplet, 1H, H4), 4.53 (t, 2H, $^3J=6.0$ Hz, C$H_2$-azole), 3.70 (t, 2H, $^3J=6.0$ Hz, C$H_2$-N-). Anal. calcd for $C_9H_{14}ClN_3O_4$: C, 40.98; H, 5.35; N, 15.93. Found: C, 41.07; H, 5.28; N, 15.50.

**Basic hydrolysis. General method.** A 1-necked round-bottomed flask was fitted with a reflux condenser and with a magnetic stirrer. The flask was charged with the corresponding ester and 0.6% NaOH (1:2 molar ratio). The mixture was left at room temperature for 24 h. After cooling water was removed in vacuo to yield quantitatively the disodium salt.

***N*-(2-Pyrazol-1-yl)ethyliminodiacetic sodium salt (1).** (From 4 to 40 mmol of diester). IR (KBr): 3130, 3100, 2960, 2940, 2870, 2840, 1730, 1600, 1505, 1425, 1395, 1345, 1300, 1205, 1180, 1140, 1115, 1090, 1055, 1030, 905, 870, 775, 740 $cm^{-1}$. $^1$H NMR ($D_2O$, δ): 7.63 (dd, 1H, $^3J_{45}=1.8$ Hz, $^4J_{35}=0.6$ Hz, H5), 7.49 (dd, 1H, $^3J_{34}=1.5$ Hz, $^4J_{35}=0.6$ Hz, H3), 6.26 (apparent triplet, 1H, H4), 4.21 (t, 2H, $^3J=6.7$ Hz, C$H_2$-azole), 3.09 (s, 4H, C$H_2$-CO-), 2.98 (t, 2 H, $^3J=6.7$ Hz, C$H_2$-N-).

***N*-2-(3,5-Dimethylpyrazol-1-yl)ethyliminodiacetic sodium salt (2).** (From 0.353 to 0.706 mmol of diester). IR (KBr): 2980, 2950, 2920, 2880, 2830, 1600, 1550, 1420, 1350, 1300, 1260, 1230, 1200, 1140, 1095, 1040, 1010, 1000, 920, 940, 900, 825, 770 $cm^{-1}$. $^1$H NMR ($D_2O$, δ): 5.85 (s, 1H, H4), 4.04 (t, 2H, $^3J=7.5$ Hz, C$H_2$-azole), 3.16 (s, 4H, C$H_2$-CO-), 2.90 (t, 2H, $^3J=7.5$ Hz, C$H_2$-N-), 2.17 (s, 3H, $CH_3$-5-), 2.07 (s, 3H $CH_3$-3-).

***N*-2-(Indazol-1-yl)ethyliminodiacetatic sodium salt (3).** (For 0.492 mmol of diester). IR (KBr): 3090, 3050, 2940, 2920, 2870, 2830, 1600, 1460, 1430, 1350, 1330, 1315, 1300, 1250, 1210, 1180, 1140, 1070, 1005, 940, 905, 880, 830, 795, 740 $cm^{-1}$. $^1$H NMR ($D_2O$, δ): 8.02 (d, 1H, $^5J_{37}=1.0$ Hz, H3), 7.75 (ddd, 1H, $^3J_{45}=8.1$ Hz, $^4J_{46}=1.1$ Hz, $^5J_{47}=1.0$ Hz, H4), 7.57 (dddd, 1H, $^3J_{67}=7.8$ Hz, $^4J_{57}=0.9$ Hz, $^5J_{47}=1.0$ Hz, $^5J_{37}=1.0$ Hz, H7), 7.43 (ddd, 1H, $^3J_{67}=7.8$ Hz; $^3J_{56}=6.8$ Hz, $^4J_{46}=1.1$ Hz, H6), 7.14 (ddd, 1H, $^3J_{45}=8.1$ Hz; $^3J_{56}=6.8$ Hz, $^4J_{57}=0.9$ Hz, H5) 4.46 (t, 2H, $^3J=7.0$ Hz, C$H_2$-azole), 3.14 (s, 4H, C$H_2$-CO-), 3.04 (t, 2H, $^3J=7.0$ Hz, C$H_2$-N-).

***N*-2-(Indazol-2-yl)ethyliminodiacetic sodium salt (4).** (For 0.492 mmol of diester). IR (KBr): 3110, 3070, 2950, 2920, 2870, 2830, 1600, 1510, 1430, 1350, 1300, 1225, 1160, 1140, 1045, 1005, 980, 940, 905, 840, 775, 755 $cm^{-1}$. $^1$H NMR ($D_2O$, δ): 8.29 (d, 1H, $^5J_{37}=0.9$ Hz, H3), 7.71 (ddd, 1H, $^3J_{45}=8.4$ Hz, $^4J_{46}=1.1$ Hz, $^5J_{47}=1.0$ Hz, H4), 7.57 (dddd, 1H, $^3J_{67}=8.7$ Hz, $^4J_{57}=1.0$ Hz, $^5J_{47}=1.0$ Hz, $^5J_{37}=0.9$ Hz, H7), 7.31 (ddd, 1H, $^3J_{67}=8.7$ Hz, $^3J_{56}=6.6$ Hz, $^4J_{46}=1.1$ Hz, H6), 7.08 (ddd, 1H, $^3J_{45}=8.4$ Hz, $^3J_{56}=6.6$ Hz, $^4J_{57}=1.0$ Hz, H5), 4.74 (t, 2H, $^3J=6.8$ Hz, C$H_2$-azole), 4.51 (t, $^3J=6.8$ Hz, C$H_2$-N).

**Determination of relaxivities.** $^1$H NMR relaxation times $T_1$ and $T_2$ (25 °C, pH 8.8) of the water protons were measured at 8.4 Tesla in a Bruker AM-360 NMR spectrometer. $T_1$ or $T_2$ values were determined by the inversion recovery method or the spin echo sequence using not less than 15 different τ values. At least six different measurements of $T_1$ or $T_2$ were performed in every sample and the results were expressed as mean ± standard deviation. Typically, 10 mM compounds **1–4** and IDA or 1 mM EDTA were dissolved in 100 mM Tris/HCl, 155 mM NaCl containing or not 0.5 mM Gd(III). Relaxivities $R_{1(2)}$ were calculated according to the expression:

$$R_{1(2)} = \Delta 1/T_{1(2)}/[M]$$

where, for every complexone, $\Delta$ is the difference in relaxation rates $1/T_{1(2)}$ of the water protons in the presence and absence of Gd(III), and [M] is the molar concentration of Gd(III).

**Magnetic resonance imaging.** $^1$H MRI was performed at 8.4 T on a Bruker AM-360 spectrometer equipped with a microscopic imaging accessory. A commercial 5 mm $^1$H microimaging probe was used. A spin echo sequence (90−τ−180−acquire) consisting of 90° nonselective pulse (8 μs) and a slice selective 180° (4 ms) refocussing pulse in the presence of a slice gradient (5 gauss/cm) was used. The echo was collected in the presence of a read gradient (15 gauss/cm) and phase encoding was induced with 64 increases of the phase gradient (from −10.7 to +10.7 gauss/cm). Pixel resolution (x, y, z) was 78 μ, 78 μ, 1 mm.

**Determination of apparent stability constants.** Apparent stability constants K′ (25 °C, pH 6.7, 0.1 M $NH_4Cl$) for Gd(III) of ArsIII and the different complexones were determined spectrophotometrically at 680 nm monitoring the increase in concentration of the ArsIII-Gd(III) complex ($\varepsilon = 1.888 \cdot 10^4\ M^{-1}\ cm^{-1}$). Solutions contained 20 mM HEPES (pH 6.7), 100 mM $NH_4Cl$, 0.1 mM ArsIII, titrating the Gd(III) concentration up to 200 μM in 5 μM steps. Binding simulations and non linear least squares regressions were programmed using the Mathematica v3.0 program (Wolfram Research Inc.) implemented on a MacIntosh Power PC platform using the models and equations described by Wells.[33] To obtain the ArsIII-Gd(III) apparent stability constant ($K'_1$), binding isotherms were fitted to a quadratic equation of the type $x^2 + \varphi_1 x + \varphi_2 = 0$, where $\varphi_1 = -([ArsIII]_t + [Gd(III)]_t + K'_1)$ and $\varphi_2 = [ArsIII]_t[Gd]_t$. Apparent stability constants (K′) for Gd(III) of compounds **1–4**, IDA, and EDTA were determined subsequently by competition with ArsIII. Briefly, the concentration of ArsIII-Gd(III) complex was determined in solutions prepared as above but containing 10 mM IDA, 10 mM compounds **1–4** or 1 mM EDTA. The sigmoidal behavior obtained in the complexones was best described considering two binding sites for Gd(III). One high affinity binding site competitive with ArsIII ($K'_2$) and one low affinity binding site non competitive with ArsIII ($K'_3$). The following simultaneous equilibria satisfy the behavior of this system: $x/(a-x-y)(b-x) = K'_1$, $y/(a-x-y)(c-y) = K'_2$, $z/(a-z)(d-z) = K'_3$; where x, y or z are the equilibrium concentrations of ArsIII-Gd(III) complex, high affinity binding sites-Gd(III) complexes or low affinity binding sites Gd(III) complexes, respectively. The total concentration of Gd(III) is denoted by a ($0 < a < 200$ μM), b refers to the total concentration of ArsIII (100 μM), c is the total concentration of complexone high affinity binding sites and d the total concentration of low affinity binding site. For the known or estimated values of a, b, c, d, and $K'_1$ the system can be solved for x, y, and z adjusting iteratively the values of $K'_2$ and $K'_3$ until the calculated value of x best fits the experimental data. The apparent stability constants of complexones **1–4**, IDA, and EDTA for $Ca^{2+}$ were determined potentiometrically with a $Ca^{2+}$ selective electrode (Ingold, Switzerland). Measurements of free $Ca^{2+}$ concentrations were performed in solutions containing 20 mM Tris/HCl buffer (pH 9.0), 100 mM $NH_4Cl$ and 1 mM $CaCl_2$ increasing concentrations of the different compounds.

**Theoretical calculations.** Semiempirical studies of chelation with different cations were performed using the Spartan 4.1.1. program implemented in a Silicon Graphics platform. The method used Parametrization Model 3 (including parameters for transition metals (PM3tm) in gas phase because parameters for metals in water were not available). The studies assume a basic pH 7 to 11 at which EDTA chelates totally in the deprotonated form ($Y^{4-}$) and in the monoprotonated form ($HY^{3-}$).

**Toxicity assays.** Toxicity was assayed by measuring the release to the medium of lactic dehydrogenase (LDH) from cultures of H35 hepatoma cells. Cells were grown until confluence in DMEM medium containing 10% fetal calf serum. Cultures were incubated in the presence of increasing concentrations of compounds **1–4**, IDA, or EDTA in the absence and presence of Gd(III). When present, Gd(III) was added to a final amount representing 10% of the total complexone concentration. The amount of LDH released to the medium at 1, 2, 3, and 6 h was measured spectrophotometrically (340 nm) using an incubation mixture containing 50 mM phosphate buffer (pH 7.2), 10 mM pyruvate and 0.5 mM NADH. At the end of the experiment cells were broken by freeze thawing three times and the total releasable LDH determined. The results obtained at every time point were expressed as percentage of the total releasable LDH after cell destruction.

## Acknowledgements

This work was supported in part by grants D.G.I.C.Y.T (PB-93-0037, PB-94-0011 and Acciones Integradas HA95-14B and HA96-99B), D.G.E.S. PB96-011-C01, PB96-0864-CO2-02), Community of Madrid (AC-07/105/96, AC-08.1/0023/97). PL received F.P.U. (Formación de Profesorado Universitario) fellowship from the Spanish Ministry of Education and Science. CGS received postdoctoral fellowships from the Deutsche Forschungsgemeinschaft and Community of Madrid.

## References

1. Tweedle, M. F.; Brittain, H. G.; Eckelman, W. C.; Gaughan, G. T.; Hagan, J. J.; Wedeking, P. W.; Runge, V. M. In *Magnetic Resonance Imaging*, 2nd ed.; Partain, C. L., Price, R. R., Patton, J. A., Kulkarni, M. V., James, A. E. W. B., Eds.; Saunders: Philadelphia, 1988; pp 793–809.
2. Peters, J. A.; Huskens, J.; Raber, D. J. *Progress NMR Spectroscopy* **1996**, *28*, 283.
3. Wood, M. L.; Hardy, P. A. J. *Magn. Reson. Imaging* **1993**, *3*, 149.
4. Lauffer, R. B. *Chem. Rev.* **1987**, *87*, 901.
5. Geraldes, C. F. G. C.; Sherry, A. D.; Lázár, I.; Miseta, A.; Bogner, P.; Berenyi, E.; Sumegi, B.; Keifer, G. E.; McMillan, K.; Maton, F.; Muller, R. N. *Mag. Res. Med.* **1993**, *30*, 696.

6. Petré, C.; Ni, Y.; Marchal, G.; Jie, Y.; Wevers, M.; Lauffer, R. B.; Baert, A. L. *Mag. Res. Med.* **1995**, *35*, 532.
7. Saeed, M.; Wendland, M. F.; Masui, T.; Higgins, C. B. *Mag. Res. Med.* **1994**, *31*, 31.
8. Anderegg, G. In *Comprehensive Coordination Chemistry*; Wilkinson, G., Gillard, R. D., McCleverty J. A., Eds.; Pergamon: New York, 1987; Vol. 2, pp 777–792.
9. Jones, C. J. In *Comprehensive Coordination Chemistry*; Wilkinson, G., Gillard, R. D., McCleverty J. A., Eds.; Pergamon: New York, 1987, Vol. 6, pp 881–1009.
10. Andrew, E. R.; Byder, G.; Griffiths, J.; Iles, R.; Styles, P. *Clinical Magnetic Resonance Imaging and Spectroscopy*. John Wiley & Sons: New York, 1990.
11. Berners-Price, S. J.; Sadler, P. J. *Coord. Chem. Rev.* **1996**, *151*, 1.
12. Steel, P. G. *Coord. Chem. Rev.* **1990**, *106*, 227.
13. Sorrell, T. N. *Tetrahedron* **1989**, *45*, 3.
14. Sadimenko, A. P.; Basson, S. S. *Complexes of pyrazoles. Coord. Chem. Rev.* **1996**, *147*, 247.
15. Mukkala, V. M.; Kankare, J. *Helv. Chim. Acta* **1992**, *75*, 1578.
16. Mukkala, V. M.; Kwiatkowski, J.; Kankare, J.; Takalo, H. *Helv. Chim. Acta*, **1993**, *76*, 893.
17. Ruloff, R.; Arnold, K.; Beyer, L.; Dietze, F.; Gründer, W.; Wagner, M.; Hoyer, E. *Z. Anorg. Allg. Chem.* **1995**, *621*, 807.
18. Wagner, M.; Ruloff, R.; Hoyer, E.; Gründer, W. *Z. Naturforch.* **1997**, *52c*, 508.
19. López Gallego-Preciado, M. C.; Ballesteros, P.; Claramunt, R. M.; Cano, M.; Heras, J. V.; Pinilla, E.; Monge, A. *J. Organomet. Chem.* **1993**, *450*, 237.
20. Ballesteros, P.; López, C.; López, C.; Claramunt, R. M.; Jiménez, J. A.; Cano, M.; Heras, J. V.; Pinilla, E.; Monge, A. *Organometallics*, **1994**, *13*, 289.
21. López, M. C.; Claramunt, R. M.; Ballesteros, P. *Heterocycles* **1994**, *37*, 891.
22. Rosen, B. R.; Belliveau, J. W.; Nevea, J. M.; Brady, T. *Mag. Res. Med.* **1990**, *14*, 249.
23. Canty, A. J.; Honeymnan, R. T. *J. Organomet. Chem.* **1990**, *387*, 247.
24. Ochi, H.; Miyasaka,T.; Arakawa, K. *Yakugaku Zasshi* **1978**, *98*, 165. *Chem. Abst.*, **1978**, *89*: 24213k.
25. Torres, J.; Lavandera, J. L.; Cabildo, P.; Claramunt, R. M.; Elguero, J. *J. Heterocycl. Chem.* **1988**, *25*, 771.
26. Koelsch, C. F.; Robinson, F. M. *J. Org. Chem.* **1956**, *21*, 1211.
27. Schwarzenbach, G.; Anderegg, G.; Schneider, W.; Senn, H. *Helv. Chim. Acta* **1955**, *38*, 1147.
28. Scarpa, A. *Methods Enzymol.* **1979**, *56*, 301.
29. Wenzel, T. *NMR Shift Reagents*; CRC: Boca Raton, 1987.
30. Koenig, S. H.; Brown, R. D. *Relaxivity of MRI magnetic contrast agents. Concepts and principles in Handbook of metal-ligand interactions in biological fluids*; 1995; Vol. 2, Part 4, pp 1093–1108.
31. Desreux, J. F.; Jacques, V. *Role of metal-ligand interactions in the design of MRI contrast agents. Concepts and principles in Handbook of metal-ligand interactions in biological fluids*; 1995, Vol. 2, Part 4, pp 1109–1118.
32. Hoard, J. L.; Lee, B.; Lind, M. D. *J. Am. Chem. Soc.* **1965**, *87*, 1612.
33. Wells, J. W. Analysis and interpretation of binding at equilibrium. In *Receptor Ligand Interactions. A Practical Approach*; Hulme, E. C., Ed.; IRL: Oxford, 1992; pp 289–395.